Using different size fractions to source fingerprint fine-grained channel bed sediment in a large drainage basin in Iran

Kazem Nosrati, Mojtaba Akbari-Mahdiabad, Peter Fiener, Adrian L. Collins

Angaben zur Veröffentlichung / Publication details:

Nosrati, Kazem, Mojtaba Akbari-Mahdiabad, Peter Fiener, and Adrian L. Collins. 2021. "Using different size fractions to source fingerprint fine-grained channel bed sediment in a large drainage basin in Iran." *CATENA* 200: 105173. https://doi.org/10.1016/j.catena.2021.105173.

Using different size fractions to source fingerprint fine-grained channel bed sediment in a large drainage basin in Iran

Kazem Nosrati [a,*], Mojtaba Akbari-Mahdiabad [a], Peter Fiener [b], Adrian L. Collins [c,*]

[a] Department of Physical Geography, School of Earth Sciences, Shahid Beheshti University, 1983969411 Tehran, Iran
[b] Water and Soil Resources Research, Institut für Geographie, Universität Augsburg, Germany
[c] Sustainable Agriculture Sciences Department, Rothamsted Research, North Wyke, Okehampton EX20 2SB, UK

Keywords:
Geochemical tracers
Weathering index of Parker
Modified MixSIR
Sediment fingerprinting
Spatial sources

A B S T R A C T

Sediment fingerprinting in data sparse regions, such as the mountainous areas of Iran, is more suited to a confluence-based sample design wherein tributary sub-basins are characterised by sediment samples using different size fractions. Our objective was therefore to fingerprint spatial source contributions to the < 37 and 37–63 μm fractions of fine-grained channel bed sediment samples collected in a large erodible mountainous river basin in Iran based on a number of statistical and machine learning approaches. Geochemical elements were measured in channel bed surface drape sediments from seven sub-basins and in delivered sediments from the basin outlet. A Bayesian mass balance model (modified MixSIR) was applied to apportion sub-basin spatial sources with four composite signatures selected using the different statistical approaches. For the < 37 and 37–63 μm fractions, the signatures all indicated that sub-basins 3 (Andajroud; 46.7%) and 7 (Ninehroud; 36.8%) were the dominant spatial sources of the fine-grained bed drape sediment samples, respectively, identifying the most active erosional zones spatially. The statistical error between known and predicted spatial source contributions using virtual mixture tests for both size fractions demonstrated the importance of using multiple different composite fingerprints to decrease the model prediction uncertainties. Despite the difficult terrain in such data sparse areas, the source fingerprinting approach provides a basis for assembling new evidence which, in turn, is of interest to scientists and managers alike.

1. Introduction

Accelerated erosion and sediment delivery rates are causing detrimental on-site and off-site impacts around the world, including land and water quality degradation, reduced crop yields and siltation of watercourses and reservoirs, with concomitant impacts on aquatic ecology and water treatment costs (Borrelli et al., 2017; Guerra et al., 2017; Pimentel and Burgess, 2013; Wilkes et al., 2019). Understanding the key sources of sediment therefore remains a critical need for policymakers, environmental agencies and basin managers to target the selection of appropriate mitigation measures for implementation on the ground.

Conventional approaches for sediment source monitoring are costly and impractical to deploy at large scales (Collins and Walling, 2004; Loughran and Campbell, 1995). The uptake of source fingerprinting has therefore accelerated over the last decade (Owens et al., 2016; Tang et al., 2019; Walling, 2013; Walling and Foster, 2016; Walling and Collins, 2016). Various tracers can be used to distinguish potential sources of sediment meaning that the fingerprinting approach is sufficiently flexible to deliver robust results in a wide range of geographical contexts (Bahadori et al., 2019; Chen et al., 2017; Collins et al., 2017; D'Haen et al., 2013; Haddadchi et al., 2013; Miller et al., 2015; Minella et al., 2008; Nosrati et al., 2011; Owens et al., 2016; Palazón and Navas, 2017; Tiecher et al., 2015; Walling, 2005; Walling and Collins, 2008). In short, fingerprinting procedures comprise two fundamental steps: source discrimination and source ascription. The former frequently relies on statistical procedures to identify the best subset of tracers or so-called composite signatures. For the latter, mass balance un-mixing models are used to determine the proportions contributed by distinguishable sources to target sediment samples collected downstream of those sources (Collins et al., 2017; Owens et al., 2016). Previous work using un-mixing models has applied either frequentist or Bayesian approaches (Collins et al., 1997a; Davies et al., 2018; Devereux et al., 2010; Haddadchi et al., 2014; Hughes et al., 2009; Sanisaca et al., 2017; Upadhayay et al., 2020). In the case of Bayesian approaches, one

* Corresponding authors:.
E-mail addresses: k_nosrati@sbu.ac.ir (K. Nosrati), adrian.collins@rothamsted.ac.uk (A.L. Collins).

available model is Modified MixSIR (Nosrati, 2017; Nosrati and Collins, 2019a; Nosrati et al., 2018; Nosrati et al., 2019; Nosrati et al., 2014) and these studies provide more detail on the statistical approaches presented herein as well as valuable background information as to how weathering indices can be used in sediment source tracing investigations.

Sediment source apportionment can be a challenging task given the spatio-temporal variation in soil erosion and the increasing complexities of erosion and sediment delivery with increasing basin scale. As one practical means of simplifying such complexity within the context of assessing sampling needs, sediment source fingerprinting procedures can adopt a sample design wherein landscape spatial units are characterised by targeted sediment sampling. Here, sediment sampling is used to provide spatially- and temporally-lumped characterisation of the properties of sediment delivered from different landscape units. Clearly, such an approach potentially reduces detail on temporal variability in tributary sub-basins sediment sources (Gellis et al., 2017). Where these units are arranged according to tributary sub-basins, the sampling design is commonly referred to as the confluence-based approach. This sample design has been used in various settings around the world (Collins et al., 1996; Collins et al., 1997b; Habibi et al., 2019; Nosrati et al., 2018; Stone et al., 2014; Vale et al., 2016; Walling et al., 1999; Zhang et al., 2012). Adoption of this approach relies upon a comparison between the tributary sub-basin sediment samples, which are used to represent source end members, and target sediment samples that are located downstream thereof on the main river stem (the overall basin outlet), encompassing contributions from the upstream spatial sources. Since this design comprises comparison of upstream and downstream sediment samples, as opposed to soil and sediment samples, as per the vast majority of source fingerprinting studies focused on establishing sediment source types rather than spatial sources, some of the complexities associated with selective erosion and transport over and along hillslopes are reduced. Another advantage is that in data sparse locations, the confluence-based approach can provide a highly pragmatic means of overcoming a lack of conventional hydrological monitoring data for sediment losses from different sub-basins within erodible drainage basins (Furuichi et al., 2016).

In previous studies, Nosrati et al. (2018) and .(2019) reported work on fingerprinting sub-basin suspended sediment sources and showed that source tracing studies should deploy a number of composite signatures selected using a combination of independent statistical tests (e.g., Kruskal–Wallis H-test, KW-H; discriminant function analysis, DFA; principal components & classification analysis, PCCA, and; general classification and regression tree models, GC&RT) to permit appraisal of the consistencies or otherwise in predicted source contributions based on the tracers used. In addition these recent studies tested and compared composite signatures comprising conventional geochemical tracers and alternative signatures combining geochemical properties with lithological weathering indices. Soil erosion and sediment delivery processes are selective (Koiter et al., 2013) meaning that careful evaluation of the most appropriate particle size fraction needs to be undertaken on a case by case basis. Careful selection of the most relevant particle size fraction to use is based on the target sediment samples collected. Directing due attention to the particle size issue can help decrease errors in the estimation of source contributions in geologically complex basins (Collins et al., 2020; Laceby et al., 2017). Where target sediment samples are characterised by a broad particle size range, it is informative to undertake source fingerprinting using different size fractions to ensure that any potential errors arising from particle size controls on tracers are minimised. Equally, in geologically complex basins, investigation of sub-basin spatial sources using a confluence-based sampling design is better placed to provide pragmatic evidence for the targeting of sediment control measures. Accordingly, the aim of this study was to use a confluence-based sampling strategy, elemental geochemistry, low-cost tracers, a number of statistical and machine learning approaches and different particle size fractions to quantify spatial source contributions in a large, data scarce, mountainous river basin in NW Iran.

2. Materials and methods

2.1. Study basin

The Alamut-Shahrood River drainage basin (2728 km^2) is located in NW Iran between 50° 06′ 48″ to 51° 11′ 49″E longitude and 36° 05′ 36″ to 36° 41′ 10″ N latitude (Fig. 1). The study area is mountainous, with elevations ranging from 724 to 4,341 m above sea level. Dominant slope gradients range between 30 and 65%. Land cover includes rangelands and woodlands (2488 km^2 area; 91.2%), cropped fields comprising orchards and dry land farming (221 km^2; 8.1%) and residential zones (19.1 km^2; 0.7%) (Iran Forests, Range and Watershed Management Organization; IFRWMO).

The main erodible lithologies of the geological formations in the study area are: marl, calcareous sandstone, sandy limestone, minor conglomerate, and alternation of dolomite, limestone and variegated shale (Fig. 1) (Annells et al., 1985). Soil texture is mainly clay loam (17–31% clay, 27–46% silt and 25–49% sand). Long-term (1976–2015) mean annual precipitation ranges from 333 to 517 mm (Iran Meteorological Organisation). On the basis of 41 years (1975–2015) of records from the Baghkalayeh hydrological station on the Alamut-Shahrood River (the archives of the Water Resources Research Organization, Iran), mean annual discharge is 11.12 $m^3\ s^{-1}$.

The steep slopes, potentially erodible lithologies (Fig. 2a), presence of dry-land farming systems on slopes that can cause serious degradation resulting in land abandonment (Fig. 2b), and anthropogenic effects associated with residential areas, also on steep slopes, (Fig. 2c) are all drivers for increasing erosion and sediment export in the study area. The fine-grained sediment and associated chemicals mobilised from the sources has important off-site consequences in the study area, including generating elevated sediment yields (Fig. 2d), which could decrease the storage capacity and projected life-span of the Sefidroud dam reservoir. The height and crest length of Sefidroud dam are 106 m and 425 m, respectively. The reservoir capacity was 1800 million cubic meters (MCM) at the beginning of operation. Approximately 600 MCM of this capacity is allocated for dead storage. The normal storage and the crest storage are 1276 MCM and 1760 MCM, respectively (Othman et al., 2013).

2.2. Field and laboratory work

Fine-grained sediment sequestered on the riverbed was sampled at the overall basin outlet and at the seven sub-basin outlets (Fig. 1) using a re-suspension method (Duerdoth et al., 2015). Samples collected at the most downstream site (basin outlet) were used as the target sediment for quantifying contributions from the upstream sub-basin outlets. In some previous work, such samples have been labelled ‘drape’ sediment deposits (Collins and Walling, 2007; Nosrati and Collins, 2019a; Olley et al., 2013; Walling et al., 1998). For the collection of each individual drape sediment sample, a stainless steel cylinder was pushed by hand into the fresh riverbed deposits to isolate an area of the bed for sample retrieval. The water in the cylinder was stirred using a handmade stirrer for ~2 min to resuspend all fine-grained deposits within the cylinder. Upon ~2 min of agitation, a sample was collected immediately using a 100-ml bottle. Fine-grained riverbed sediment was sampled once (on random day) at all sites in September 2018 from riffles. Based on visual observations of storm discharge the seven sampled sub-basins in the study area were the most important with respect to suspended sediment loads. In addition, prior to field sampling, the results of independent field investigations and targeted questionnaires completed by experts in the Natural Resources Bureau of Gazvin Province were also used to select potential sub-basin spatial sediment sources in the study area. Five sub-samples were collected in a ~10 m long reach (spaced at approximate 2 m intervals) at each sampling site and combined into individual composite samples. In total, five composites were sampled from each sub-basin outlet and a further eight from the most downstream sampling

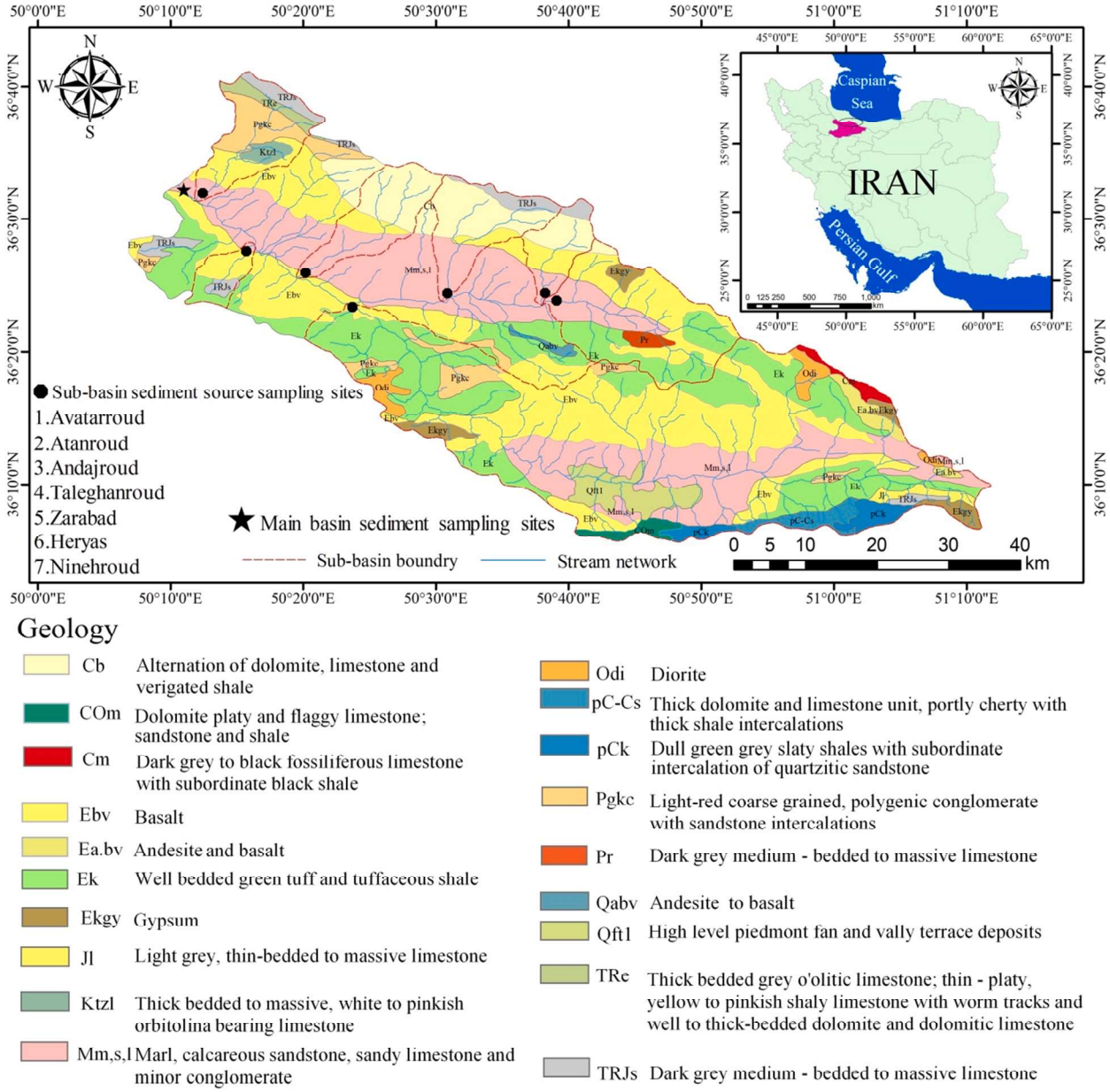

Fig. 1. Map of the Alamut-Shahrood River drainage basin, showing the location of the study basin in NW Iran, in northern Ghazvin Province, geology and sediment sampling locations in the seven representative tributary sub-basins and at the overall downstream site.

site. Oven-dried (at 40 ℃) composite samples weighed ~ 50 g each.

In order to identify the dominant particle size fraction in the riverbed sediment samples and to confirm that the tracers were present across that fraction rather than a sub-fraction, a two-step procedure was used: 1) dry sieving to fractionate the riverbed samples to 500–1000, 250–500, 125–250, 63–125, and < 63 μm, and 2) further fractionation of the dominant particle size fraction to show that the tracers were distributed across the dominant fraction rather than a sub-fraction therein. The results of the particle size assessment confirmed that the < 63 μm fraction was dominant (Figure S1). In step two, wherein the < 63 μm fraction of all riverbed sediment samples was further fractionated into < 37 and 37–63 μm, our findings suggest that the tracers we used are distributed across both of these fine-grained size fractions. Consequently, both the < 37 and 37–63 μm fractions of the sub-basin and overall outlet riverbed sediment samples were used for tracer analysis to apportion spatial sources. Fractionation can be used to help control for particle size effects on tracers.

Geochemical tracers were measured using 1 g of each sediment sample for both the < 37 and 37–63 μm fractions digested in aqua regia (HCl–HNO_3; 3:1) using a Velp Thermo-reactor at 95 °C for two hours. Extracts were filtered through S&S ME24 (0.2 μm) filter papers and elemental concentrations were measured using a Varian SpectrAA-20 Plus (Merck KGaA, Frankfurt, Germany) calibrated with a standard for Ca, Co, Fe, K, Mg, Mn, Na, Pb, Sr, and Zn. Given that aqua regia was used for the digestions, the results should be assumed to represent pseudo-total concentrations of geochemical elements in the absence of complete dissolution using a more powerful acid matrix (Queavuviller, 1998). Analytical precision was > 95% in all cases.

The weathering index of Parker (WIP; equation (1)) (Collins et al., 2020; Garzanti et al., 2016; Nosrati et al., 2019) was calculated based on elemental oxides (Eq. (1)). The ratio of Fe to Mn (Fe/Mn) was also calculated:

$$WIP = 100 \cdot (CaO/0.7 + 2Na_2O/0.35 + 2K_2O/0.25 + MgO/0.9) \quad (1)$$

Therefore, the list of potential tracers used in the statistical analysis

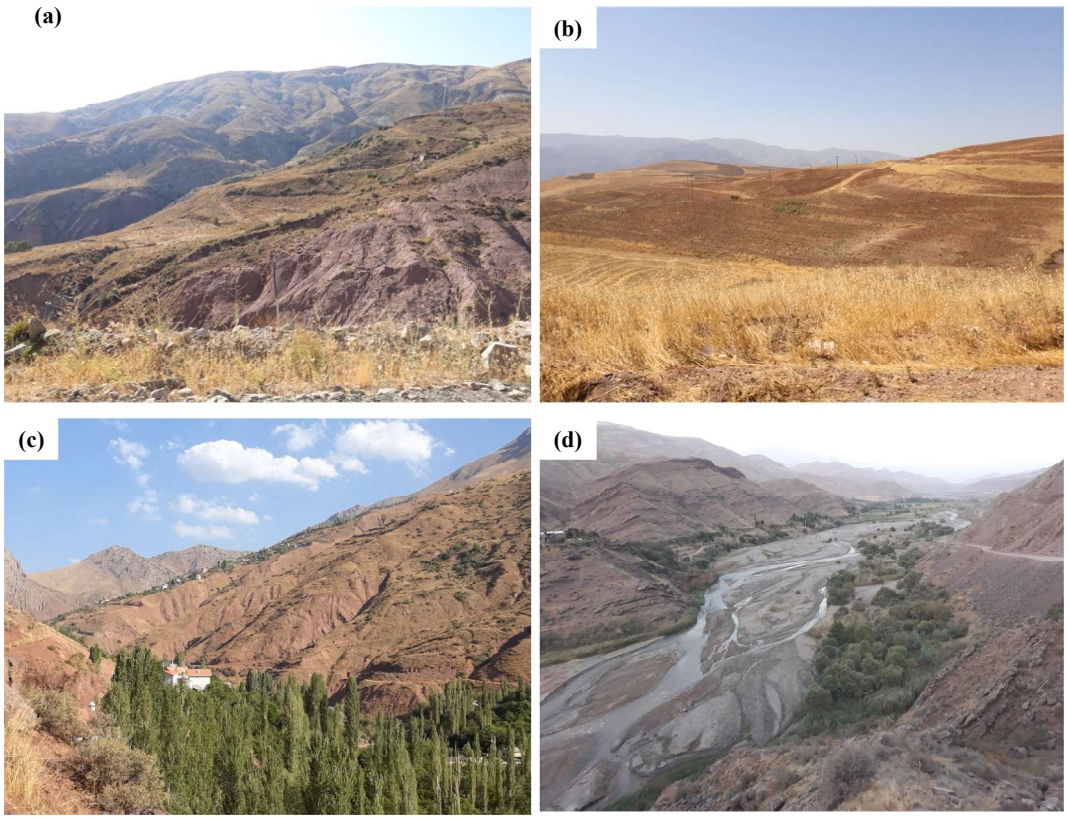

Fig. 2. Photos showing: (a) the variety of potentially erodible lithological formations; (b) dry-land farming on steep slopes; (c) residential areas on steep slopes, and; (d) off-site impacts of elevated erosion and sediment mobilisation.

for source discrimination comprised the following elements Ca, Co, Fe, K, Mg, Mn, Na, Pb, Sr, Zn, as well as WIP, and Fe/Mn ratio.

2.3. *Distinguishing spatial sediment sources*

A range test (bracket test) was used to assess the presence of significantly non-conservative tracers, wherein the tracer concentrations in the most downstream samples were compared with the corresponding ranges measured in the sub-basin samples. Tracers failing this test which is widely applied in the international literature were discarded (e.g. Nosrati et al., 2018).

Four approaches were used to test discrimination of the spatial sediment sources. These tests were: (1) the Kruskal–Wallis H-test (KW-H); (2) a combination of the KW-H and backward discriminant function analysis (DFA); (3) a combination of the KW-H and principal component & classification analysis (PCCA), and; (4) a combination of KW-H and a general classification tree model (GCTM). Each test (STATISTICA V.8.0; StatSoft, 2008) identified a composite signature. Further details concerning the application of these specific statistical tests in sediment source fingerprinting work can be found in Nosrati and Collins (2019a), Nosrati and Collins (2019b), and Nosrati et al. (2019).

2.4. *Ascribing sub-basin spatial sources*

Modified MixSIR (Nosrati et al., 2014) was used to determine spatial sediment sources using the four composite signatures. In short, modified MixSIR apportions sediment sources using probability distributions for the contributions of each individual source to the target sediment samples. Tracer distributions for the downstream sediment samples are solved using means and standard deviations of the same tracers in the tributary sub-basin spatial sources. The resampling methodology was utilised to generate 10^6 samples from the posterior distributions. Modelled source proportions from the seven sub-basin spatial sources based on each composite signature selected by different statistical approaches were compared using the root mean square error (RMSE) to assess differences between the spatial source estimates generated using each composite signature. A two-sample Wald-Wolfowitz Runs test was also used to identify statistically significant contrasts between the posterior distributions generated for the proportional contributions from the sources using each signature. This test is sensitive to differences in the frequency distributions generated by mass balance models.

In order to evaluate the modelled spatial source proportions based on each signature, virtual mixtures were used (Collins et al., 2017; Palazón et al., 2015). This step in the fingerprinting procedure was used to assess un-mixing model accuracy. The virtual sediment mixtures were: 1) equal proportions from all sources; 2) 5% sub-basin 1, 2, 3, 4, 6 and 7, 70% sub-basin 5; and 3) 5% sub-basin 1, 2, 3, 5, 6, and 7, 70% sub-basin 4. Model accuracy was quantified using the averaged root mean square error (RMSE) and mean absolute error (MAE) between the predicted and known source contributions using each of the signatures.

3. Results

3.1. *Elemental fingerprints*

Fig. 3 shows the concentrations of tracers in the source end members and overall downstream riverbed sediment samples for the < 37 and 37–63 μm fractions. All tracers passed the range test and so were retained for further analysis. Fig. 3 also shows the results of applying the KW-H test and further confirmation that the tracer contents of the spatial sources were significantly different based on a Scheffe post-hoc test. These results confirmed that all tracers returned a statistically significant difference ($p < 0.05$) between the sediment sources. All tracers were therefore included in the KW-H signatures for both particle size fractions.

The 12 statistically significant tracers from the KW-H test were

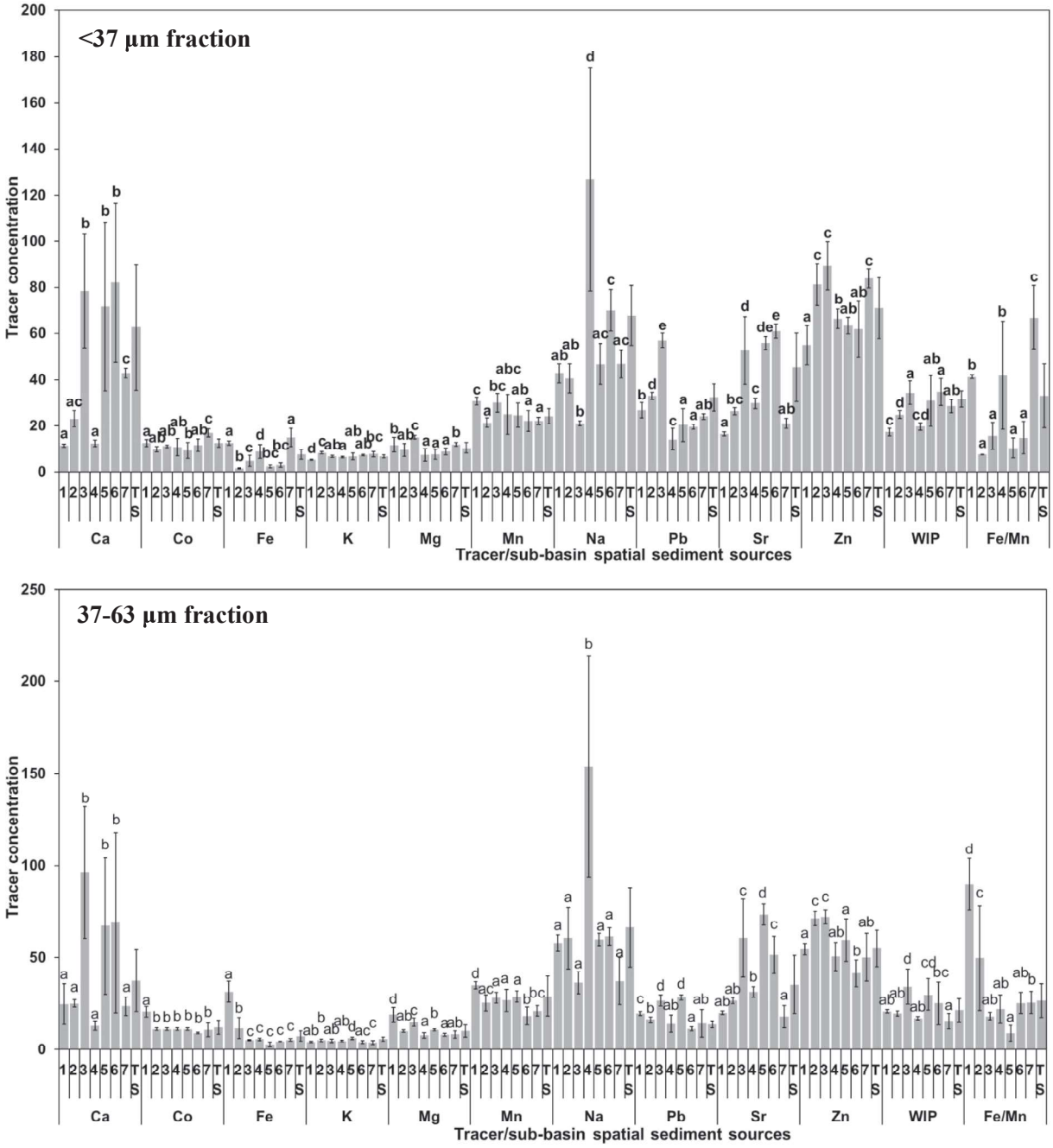

Fig. 3. Tracer concentration data for the different sub-basin spatial sediment sources and downstream target sediment samples (ST) for both particle size fractions. The units of Ca, Fe, K, Mg are g kg^{-1}. The units of Co, Pb, Mn, Na, Sr and Zn are mg kg^{-1}. For concentrations of Mn, Na, and Sr, the data on the graph should be multiplied by 10. WIP: Weathering Index of Parker. Different small letters on sub-basin bars of each tracer indicate that the tracer is significantly different at the 5% level based on a Scheffe post-hoc test.

imputed in the backward stepwise DFA (Fig. 3). For the < 37 µm fraction, the values of DFA statistics (Tables S1 and S2) confirmed that six tracers comprising Pb, Sr, Fe, Na, Fe/Mn, and WIP were selected as a composite signature. Corresponding DFA results for the 37–63 µm size fraction are also presented in Table S1 and Table S2. In this case, the composite signature combined K, Mg, Mn, Pb, Sr, Zn, Fe/Mn, and WIP. The backward stepwise DFA assigned 100% of the spatial source end member samples correctly using the selected tracers in the signatures for both particle size fractions. The DFA first and second discriminant functions illustrated that the end member riverbed sediment samples are well separated for both size fractions (Fig. 4).

Tracers identified by the KW-H as statistically significant were also tested using PCCA for both particle size fractions. For the < 37 µm fraction, four PCs explained > 80% of the variance for the nine tracers with the exception being Mn and Na. Accordingly, these tracers were the least important due to their communalities. The highly-weighted tracers representing PC1 were Ca, Fe, Sr, WIP and Fe/Mn. For PC2, the highly-weighted tracer was Mg. The highly-weighted tracer under PC3 was Mn. Under PC4, the corresponding highly-weighted tracer was Zn (Table S3).

The results of PCCA for the 37–63 µm fraction showed that the cumulative total variance for the first four PCs is > 87% (Table S3). The highly-weighted tracers under PC1 were Ca, Sr, and WIP. For PC2, the highly-weighted tracers were Co and Mg. The highly-weighted tracer under PC3 was Na, whereas it was Zn for PC4 (Table S3). The PC

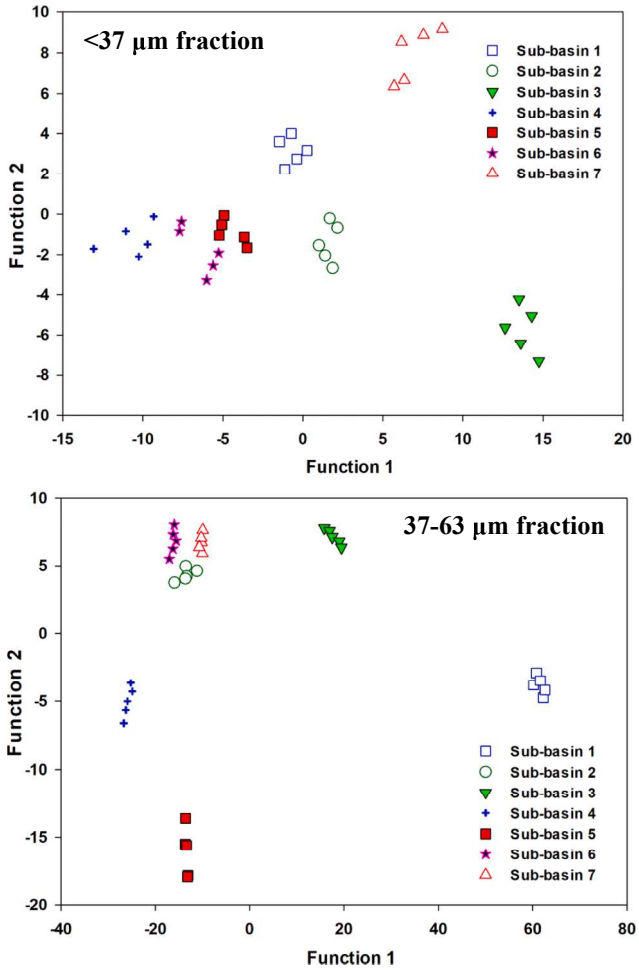

Fig. 4. Scatterplots of the first and second discriminant functions calculated using backward DFA with the composite signatures selected for both particle size fractions.

coordinates for the selected tracers for the < 37 µm and the 37–63 µm fractions were plotted in Fig. 5. Tracers related to these PCs for both particle size fractions provided additional fingerprints (for the < 37 µm fraction: Ca, Fe, Mg, Mn, Sr, Zn, WIP, Fe/Mn and for the 37–63 µm fraction: Ca, Co, Mg, Na, Sr, Zn, WIP).

During the machine learning for the < 37 µm and the 37–63 µm fractions, the 12 tracers passing KW-H were used in a GCTM. Fig. 6 shows the trees generated using the tracer concentrations in each particle size class of the source end members using a v-fold cross-validation (CV cost) test. For the < 37 µm fraction, the histograms of sediment source samples (in the terminal nodes) in the final tree (CV cost = 0.06) showed that all spatial sediment source samples were grouped significantly (Fig. 6). For the 37–63 µm fraction, the histograms of source samples per class at the terminal nodes (CV cost = 0.09) also confirmed 100% discrimination of the spatial sediment sources (Fig. 6).

The predictor (i.e., tracer) importance values for the spatial sources for the < 37 µm and the 37–63 µm fractions are displayed in Fig. 6. The tracer importance was calculated by normalizing the mean of the sums-of-squares regression for all tracers over all trees and nodes relative to the most important tracer. Therefore, the tracer importance values reveal the power of the relationship between the tracers and the spatial sediment sources. For the < 37 µm fraction, the tracers Fe, Mg, Na, Pb, and Sr (importance value ≥ 0.7) were shortlisted as important predictors. For the 37–63 µm fraction, the tracers Fe, Mg, Na, and Fe/Mn (importance value ≥ 0.9) were the best predictors.

The biplots for both size fractions in Figure S2 revealed that the

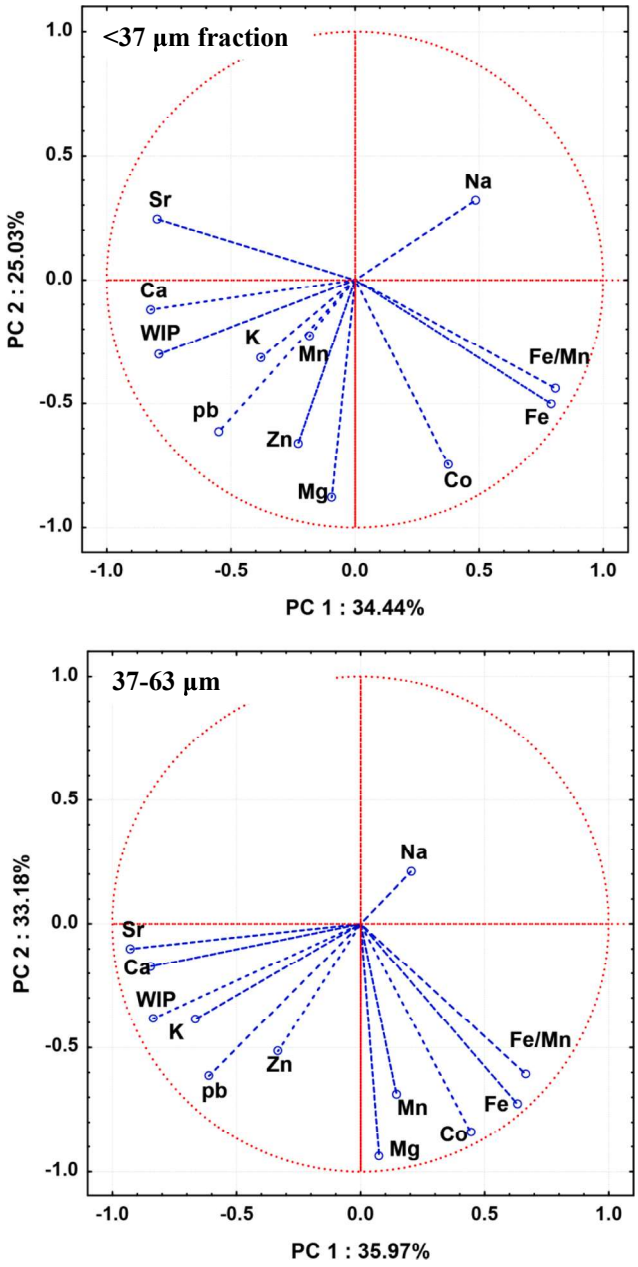

Fig. 5. Projection of the composite signatures on the PC-plane using PCCA for both particle size fractions.

tracers selected in the final signatures had not been subjected to major transformation during redistribution from the spatial source to the downstream target fine-grained channel drape bed sediment sampling locations.

3.2. *Spatial sediment sources*

For the < 37 µm fraction, the different signatures all suggested that sub-basins 3 (Andajroud) and 4 (Taleghanroud) were the dominant sources of the fine-grained drape sediment samples (the mean values ± 1 standard deviation, SD, estimated as 46.7% ± 8.4% and 39.4% ± 5.8%, respectively) (Fig. 7). For the 37–63 µm fraction, sub-basin 7 (Ninehroud with a mean ± 1 SD contribution of 36.8% ± 25.9%) was the dominant and sub-basins 3 and 4 (mean ± 1 SD contributions of 22.2% ± 14.5% and 23% ± 26.8%, respectively) were the second most important spatial sources (Fig. 7). For the < 37 µm fraction, the RMSE between the apportionment results using signatures selected by different statistical

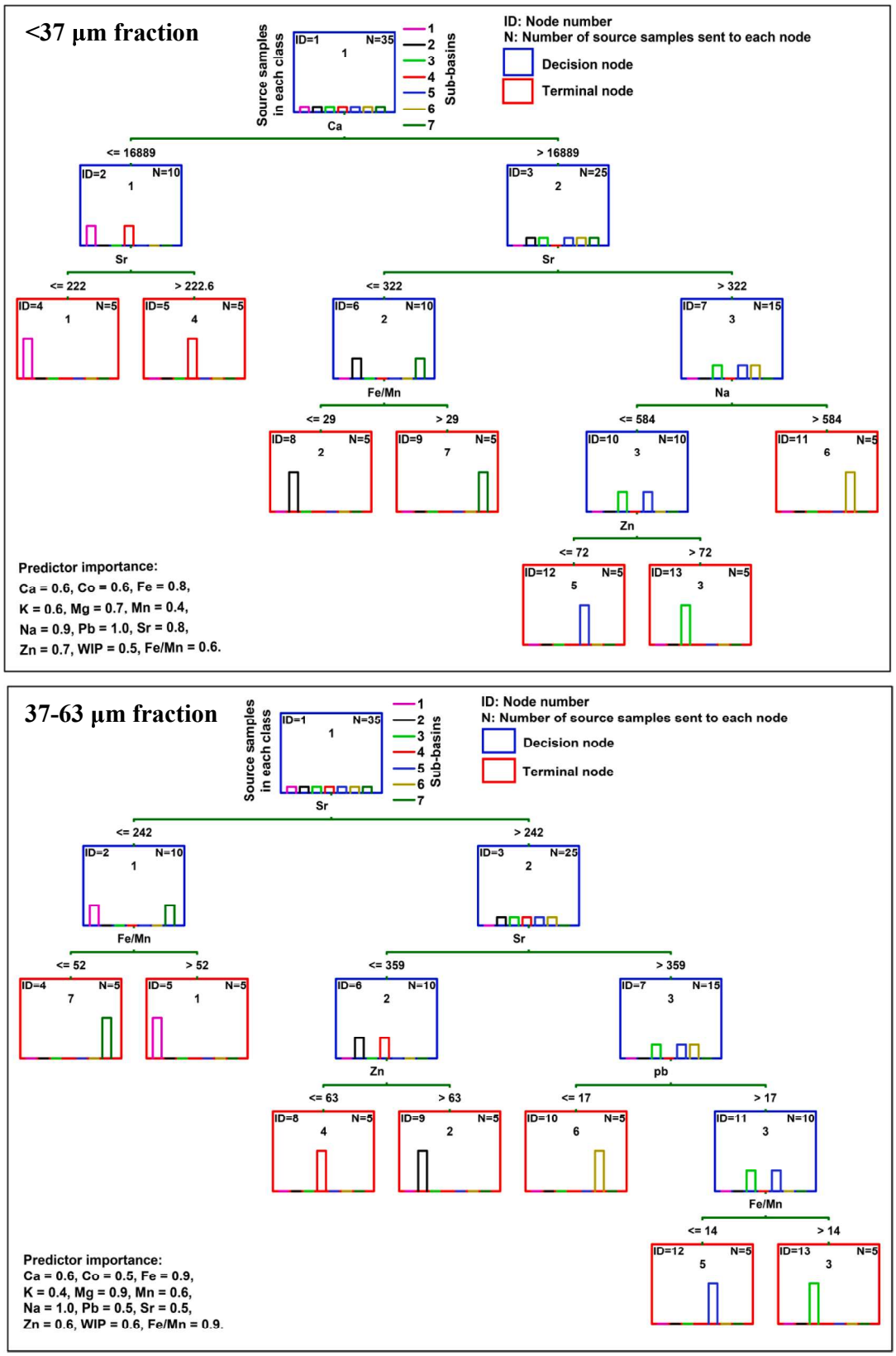

Fig. 6. Classification trees and tracer importance values for the sub-basin spatial sediment sources using GCTM for both particle size fractions. The units for all elements are mg kg^{-1}.

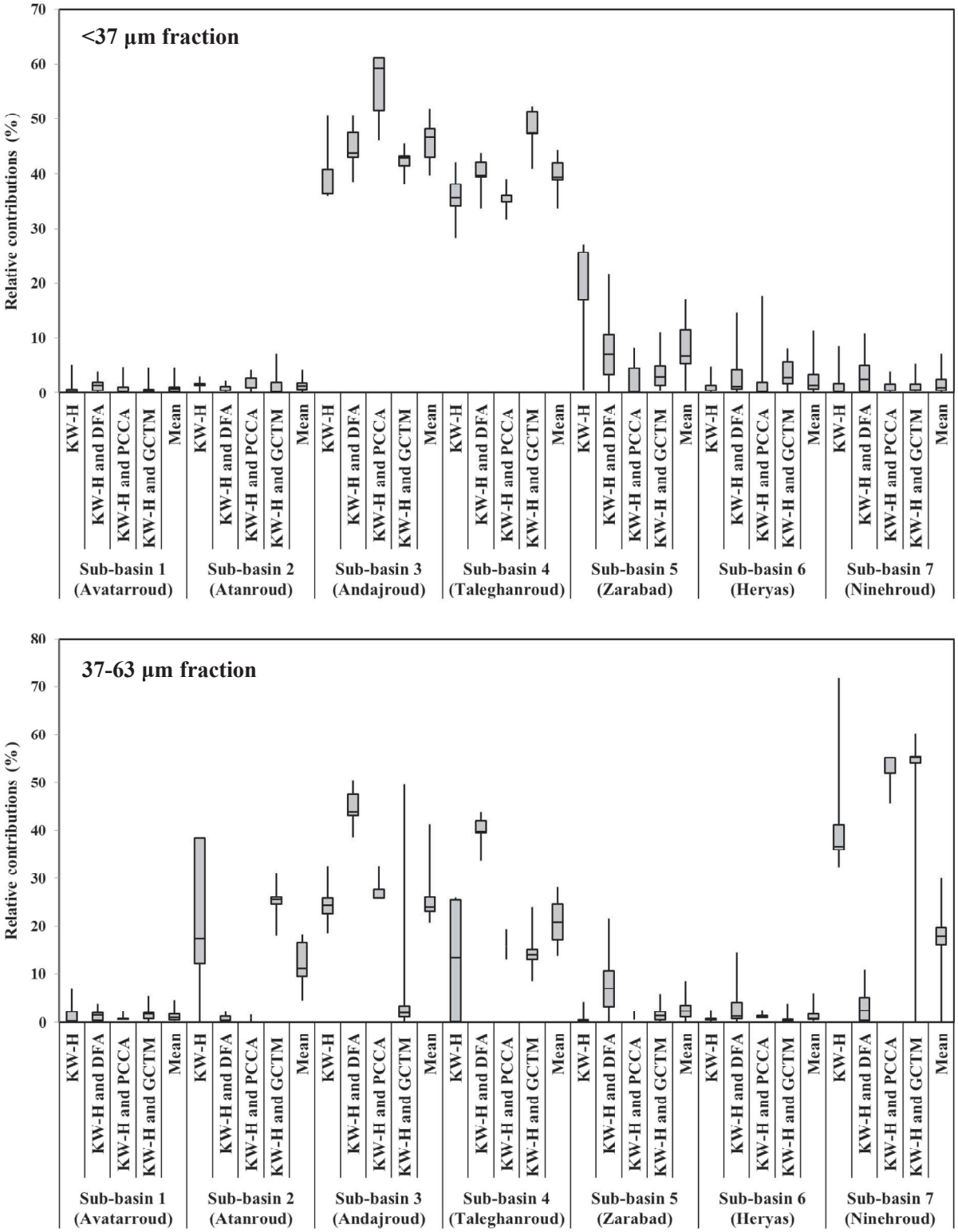

Fig. 7. Relative contributions (box plots) from the seven sub-basin spatial sources to the main stem target sediment samples for both particle size fractions using composite signatures selected by different statistical approaches.

approaches for the contributions of the seven sub-basin spatial sources to the main stem sediment samples was 0.7, 1.5, 11.0, 7.6, 9.6, 1.2, and 1.3%, respectively. For the 37–63 µm fraction, the RMSE between the apportionment results for the seven sub-basin spatial sources was 0.9, 24.8, 18.9, 35.1, 0.7, 0.4, and 33.9%, respectively.

Pairwise comparisons of the estimated source contributions using the four different signatures are presented in Table 1. A significance value of < 0.05 confirms significant differences between the two distributions. The results for the < 37 µm and 37–63 µm fractions showed that all of the pairwise comparisons were significantly different (Table 1).

Table 1
Wald-Wolfowitz Runs test pairwise comparison results (z-statistic) for the probability density functions computed for the predicted contributions from the seven sub-basin spatial sediment sources based on composite signatures selected by different statistical approaches. * p- levels are < 0.001.

Paired statistical approaches in selecting tracers	Spatial (sub-basins) sediment sources						
	1	2	3	4	5	6	7
37 μm fraction							
KW H-test vs. Combination of KW- H-test and DFA	25.2*	27.1*	27.4*	28.9*	28.4*	25.6*	25.9*
KW-H-test vs. Combination of KW -H-test and PCCA	32.6*	32.3*	34.1*	33.0*	34.4*	33.2*	32.0*
KW-H-test vs. Combination of KW -H-test and GCTM	33.2*	34.0*	34.1*	35.4*	34.9*	33.7*	33.9*
Combination of KW-H- test and DFA vs. Combination of KW-H test and PCCA	10.9*	11.4*	13.2*	12.9*	11.5*	11.4*	11.7*
Combination of KW-H- test and DFA vs. Combination of KW-H test and GCTM	11.6*	13.5*	13.0*	15.1*	12.9*	12.2*	12.2*
Combination of KW-H- test and PCCA vs. Combination of KW-H test and GCTM	15.4*	15.8*	17.7*	17.7*	16.1*	15.7*	15.7*
37–63 μm fraction							
KW H-test vs. Combination of KW- H-test and DFA	8.1*	9.7*	9.7*	9.7*	8.1*	8.1*	9.7*
KW-H-test vs. Combination of KW -H-test and PCCA	10.8*	11.1*	11.1*	10.2*	10.5*	10.5*	11.4*
KW-H-test vs. Combination of KW -H-test and GCTM	19.2*	20.1*	20.4*	19.6*	19.4*	19.4*	20.2*
Combination of KW-H- test and DFA vs. Combination of KW-H test and PCCA	3.6*	3.6*	4.4*	4.4*	4.4*	3.6*	4.4*
Combination of KW-H- test and DFA vs. Combination of KW-H test and GCTM	12.8*	15.2*	12.8*	15.2*	12.8*	12.8*	12.8*
Combination of KW-H- test and PCCA vs. Combination of KW-H test and GCTM	14.8*	17.6*	17.2*	14.0*	14.0*	14.0*	14.8*

4. Discussion

4.1. Adoption of a confluence-based sampling strategy

Our data support the use of a smaller number of accessible locations for investigating spatial sources for sediment fingerprinting in data sparse environments with challenging terrain. A confluence-based approach focuses sampling effort by permitting a small number of sampling sites to integrate the spatio-temporal variation in erosion and sediment delivery patterns. In this approach, complexities introduced by the distances between sources and receptors are reduced by sampling immediately upstream of the tributary confluence for each spatial unit, thereby providing a proxy for the tributary geochemical signature (Vale et al., 2016). On the basis of our sampling strategy, which was an initial reconnaissance survey, we do not have information on temporal variability in the sediment signatures of the tributary sub-basins, and the use of riverbed material as end members may pick up an older source signal than suspended sediment (Gellis et al., 2017). As with alternative source fingerprinting strategies, this sampling design assumes there is no significant effect resulting from potential tracer alteration processes such as selective detachment, transport or deposition between the end member and the basin outlet sampling points. Our sampling design yields a time-integrated estimate of end member and target sediment signatures and assumes bed material chemistry does not change significantly over time. Here, we point readers to other work which has used a single sampling visit to characterise bed sediment chemistry, albeit, not for source fingerprinting purposes (Horowitz et al., 2012). To support direct comparison of the end member and target riverbed sediment samples, we removed the effect of particulate size distribution as one of the main factors influencing tracer concentrations (Grygar and Popelka, 2016; Horowitz, 1991). In order to mitigate particle size effects on tracers, there are two principal approaches in sediment tracing studies comprising: using fine particle size sub-fractions (e.g., of the < 63 μm fraction) selected carefully on the basis of the d_{90} particle size for the target sediment samples and the use of more generic broader particle size fractions (e.g., the bulk < 63 μm fraction) combined with further correction factors in the un-mixing model (Collins et al., 2017; Laceby et al., 2017). Tracing different particle size sub-fractions has some advantages including: 1) decreasing potential errors produced by different particle size ranges in the samples collected to represent end members and target sediment, 2) increasing the accuracy of estimated source contributions compared with using a generic particle size fraction combined with a correction factor in the mass balance model, 3) providing a basis for assessing consistency in source estimates across size fractions. In this study, we fractionated the bed sediment samples into one additional sub-fraction since the d_{90} of the target sediment samples indicated that the < 63 μm fraction was appropriate for capturing the bulk of the fine sediment sequestered on the river bed, but in conjunction with that size range, we needed to control for any potential particle size effects on the tracers used.

There is no standard combination of statistical methods to select the composite tracers in sediment tracing so in order to test the sensitivity of estimated source ascriptions to different sets of tracers, four multivariate statistical techniques were used. Multiple different composite fingerprints can be used to identify a signature yielding the lowest prediction uncertainties and to assess consistencies in the predicted source proportions (Collins et al., 2017; Collins et al., 2012; Uber et al., 2019). For the < 37 μm fraction, the maximum RMSE between the apportionment results was 11% while for the 37–63 μm fraction, it was 35.1%. This result demonstrated that the magnitude of the difference between the spatial source proportions generated using each composite fingerprint is larger for the coarser particle size fraction. In addition, pairwise comparisons of the estimated spatial source contributions using the four different composite signatures confirmed statistically significant differences for the results specific to either the < 37 μm or 37–63 μm fractions (Table 1) and demonstrated the sensitivity of model predictions to the different composite signatures. The Kolmogorov–Smirnov test was used in a similar application in a previous paper by (Nosrati et al., 2018). The Wald-Wolfowitz test used herein has been shown to be more powerful than the Kolmogorov–Smirnov test for detecting differences between distributions if the distributions differ in variance and have at the most

only a small difference in location (Senger, 2013). This approach provides a means of identifying more than one composite signature and of assessing source prediction sensitivity to tracer choice, although the costs of elemental measurements could be increased. Since conventional field monitoring data are rarely available for testing fingerprinting predictions directly, the current recommended method for evaluating un-mixing model predictions is artificial or virtual sample mixtures (Collins et al., 2017; Gaspar et al., 2019; Haddadchi et al., 2014; Uber et al., 2019). Accordingly, mixture tests have become increasingly established in recent studies (e.g., Haddadchi et al., 2014; Mohammadi Raigani et al., 2019; Nosrati et al., 2019). The RMSE and MAE estimates based on the virtual mixture tests for the different final composite signatures for the < 37 μm fraction ranged between 1.6% – 13.2% and 1.2% – 8.3%, respectively (Table 2). The RMSE and MAE estimates based on the virtual mixture tests for the different final composite signatures for the 37–63 μm fraction ranged between 1.5–13.3% and 1.0–8.3%, respectively (Table 3). These error levels are comparable to those reported in existing literature (e.g., Brosinsky et al., 2014; Uber et al., 2019).

One of the main challenges for un-mixing models is that they cannot deterministically solve mass-balance equations when the number of sources is different from the number of tracers + 1. The use of modified MixSIR can account for this challenge. In the study reported here, the numbers of sediment sources is seven while the numbers of tracers constituting the different composite fingerprints selected by a combination of statistical techniques are between four to eight tracers for both fractions (except in the case of the signature selected using the KW-H test which included 12 tracers). Critically, the results returned acceptable errors in the context of those reported by many other fingerprinting studies.

Application of novel fingerprints continues to be a research focus for sediment source fingerprinting (Collins et al., 2020). The integrated usage of low cost and high-resolution techniques should facilitate the analysis of a large number of samples for obtaining reliable information on variations in sediment source contributions (Evrard et al., 2019). Nosrati et al. (2019) recently combined weathering indices with geochemical tracers to investigate the spatial sources of suspended sediment in northern Tehran, Iran. Indeed, there is a need to develop novel tracers from other approaches utilized in Earth System sciences (Collins et al., 2020). Selecting appropriate composite signatures using new statistical techniques (e.g., GCTM) helps to find robust subsets of lower cost tracers and may help avoid the need for alternative expensive tracers. As previous work has shown, widely used DFA may not always provide the most suitable variable selection because of collinearity between tracers (Vale et al., 2016). Regardless, it remains important to interpret the tracer sets selected statistically for composite signatures in the context of lithological and pedological patterns in the study area. In the absence of a sound physical basis for the end member discrimination yielded by particular tracers, composite signatures should be seen as statistical solutions to the sediment sourcing problem. In the case of the study herein, we are able to interpret the spatial source contributions on the basis of the lithologies present in the study area.

Using the < 37 μm fraction, fingerprinting highlighted high sediment contributions from sub-basins 3 (Andajroud; 46.7%) and 4 (Taleghanroud; 39.4%) using each of the different composite signatures. For the 37–63 μm fraction, sub-basin 7 (Ninehroud; 36.8%) was highlighted as the dominant spatial sediment source, followed by sub-basins 3 (Andajroud; 22.2%) and 4 (Taleghanroud; 23.0%). Overall these results demonstrated that three sub-basins (Andajroud, Taleghanroud, and Ninehroud) are the active spatial erosion zones and that management strategies should be focused on them.

The main lithologies of the Andajroud and Taleghanroud sub-basins include marl, calcareous sandstone, sandy limestone and minor conglomerate, plus alternating dolomite, limestone and verigated shale, all of which are sensitive to chemical weathering and the production of silt and clay. Physical weathering processes produce smaller particulate material and, based on the particle size, the surface area is exposed to chemical attack whereby silts and clays weather quickly compared with gravels and sands (Huggett, 2011). Based on the weathering zone of the study area, leaching is relatively weak (Thomas, 1994). Local factors including parent rock, topography, and vegetation play an important role in governing the weathering processes (Huggett, 2011). Lithology influences the rate of weathering with erodible lithology and steep slopes in the sub-basins highlighted by the source fingerprinting work driving higher erosion rates and sediment yields.

Table 2
Comparison of the predicted and known relative contributions from the spatial sediment sources to the virtual sediment mixtures using the composite signatures selected by different statistical approaches and the corresponding root mean squared error (RMSE) and mean absolute error (MAE) for the < 37 μm fraction.

Statistical approaches and composite fingerprints	Source proportions	Spatial (sub-basin) sediment source contributions							RMSE	MAE
		1	2	3	4	5	6	7		
KW-H(Tracers: All tracers)	Known	14.3	14.3	14.3	14.3	14.3	14.3	14.3	2.6	2.1
	Predicted	16	15.2	13	11	10.2	17.9	14.2		
	Known	5.0	5.0	70.0	5.0	5.0	5.0	5.0	3.1	2.1
	Predicted	6.1	8.2	62.9	2.9	5	5.8	4.7		
	Known	5.0	5.0	5.0	70.0	5.0	5.0	5.0	8.2	5.5
	Predicted	13.8	8.4	2.9	50.8	6.3	7	6.8		
Combination of KW-H and DFA (Tracers: Fe, Na, Pb, Sr, WIP, Fe/Mn)	Known	14.3	14.3	14.3	14.3	14.3	14.3	14.3	3.0	2.8
	Predicted	17.5	12.8	12.5	10.8	11	18.7	12.1		
	Known	5.0	5.0	70.0	5.0	5.0	5.0	5.0	3.0	1.8
	Predicted	5.8	7	62.8	2.9	5.1	4.7	4.8		
	Known	5.0	5.0	5.0	70.0	5.0	5.0	5.0	8.7	5.7
	Predicted	12.7	6.4	2.8	49	7.4	7.5	7.8		
Combination of KW-H and PCCA (Tracers: Ca, Fe, Mg, Mn, Sr, Zn, WIP, Fe/Mn)	Known	14.3	14.3	14.3	14.3	14.3	14.3	14.3	1.6	1.2
	Predicted	14.9	14	12.7	11.1	12.7	15.3	14.7		
	Known	5.0	5.0	70.0	5.0	5.0	5.0	5.0	6.1	3.7
	Predicted	6.5	8	54.5	3.9	6	7.7	6.1		
	Known	5.0	5.0	5.0	70.0	5.0	5.0	5.0	13.2	8.3
	Predicted	19.6	10.2	4.3	38.9	8.2	6.3	7.3		
Combination of KW-H and GCTM (Tracers: Fe, Mg, Na, Pb, Sr)	Known	14.3	14.3	14.3	14.3	14.3	14.3	14.3	1.9	1.6
	Predicted	14.6	12.1	12.9	11.2	12.5	16.9	14.1		
	Known	5.0	5.0	70.0	5.0	5.0	5.0	5.0	2.6	1.6
	Predicted	5.2	6.7	63.6	2.9	4.8	5.2	4.8		
	Known	5.0	5.0	5.0	70.0	5.0	5.0	5.0	9.2	6.1
	Predicted	10.1	6.9	2.8	47.2	7.9	7.9	10.1		

Table 3
Comparison of the predicted and known relative contributions from the spatial sediment sources to the virtual sediment mixtures using the composite signatures selected by different statistical approaches and the corresponding root mean squared error (RMSE) and mean absolute error (MAE) for the 37–63 μm fraction.

Statistical approaches and composite fingerprints	Source proportions	Spatial (sub-basin) sediment source contributions							RMSE	MAE
		1	2	3	4	5	6	7		
KW-H(Tracers: All tracers)	Known	14.3	14.3	14.3	14.3	14.3	14.3	14.3	1.5	1.0
	Predicted	14.6	14.7	12.9	14.5	15.1	14.4	10.8		
	Known	5.0	5.0	70.0	5.0	5.0	5.0	5.0	7.5	4.7
	Predicted	5.8	6.3	53	3.3	14.7	6.3	5.8		
	Known	5.0	5.0	5.0	70.0	5.0	5.0	5.0	6.8	4.4
	Predicted	4.8	9.5	4.1	53.6	6.6	6.6	10.5		
Combination of KW-H and DFA (Tracers: K, Mg, Mn, Pb, Sr, Zn, WIP, Fe/Mn)	Known	14.3	14.3	14.3	14.3	14.3	14.3	14.3	1.5	1.1
	Predicted	15.1	13.9	12.7	14.7	14.9	13.6	10.8		
	Known	5.0	5.0	70.0	5.0	5.0	5.0	5.0	9.5	5.3
	Predicted	7	6.8	48.1	5.2	17	4.6	5.3		
	Known	5.0	5.0	5.0	70.0	5.0	5.0	5.0	13.3	8.3
	Predicted	4.9	11.1	4.7	38.1	7.8	10.2	16.8		
Combination of KW-H and PCCA (Tracers: Ca, Co, Mg, Na, Sr, Zn, WIP)	Known	14.3	14.3	14.3	14.3	14.3	14.3	14.3	2.5	2.1
	Predicted	13.7	17.7	11.9	13.5	15.5	12.3	9.7		
	Known	5.0	5.0	70.0	5.0	5.0	5.0	5.0	7.8	4.8
	Predicted	5.8	9.6	51.2	3	11.4	5.7	5.6		
	Known	5.0	5.0	5.0	70.0	5.0	5.0	5.0	7.3	4.5
	Predicted	5.1	11.9	3.7	52.5	6	6.1	8.5		
Combination of KW-H and GCTM (Tracers: Fe, Mg, Na, Fe/Mn)	Known	14.3	14.3	14.3	14.3	14.3	14.3	14.3	2.4	2.0
	Predicted	15	11	11.3	12.3	13.1	13.9	10.6		
	Known	5.0	5.0	70.0	5.0	5.0	5.0	5.0	7.5	4.6
	Predicted	5.5	4.9	51.7	3.6	10.8	7.1	9.2		
	Known	5.0	5.0	5.0	70.0	5.0	5.0	5.0	10.4	6.0
	Predicted	5	7.1	5.6	43.8	8	10.8	9.4		

4.2. Implications for sediment management

Because it is impossible to prevent soil erosion completely, extreme soil erosion should be decreased to manageable levels to diminish on-site and off-site unintended consequences. Knowledge of tributary sub-basin source contributions is a pragmatic approach to understanding the coarse resolution spatial distribution of source erosion at large basin scale for developing management strategies. In this study, sub-basins 3, 4 and 7 need to be targeted for sediment control. Source tracing fine-grained channel bed sediment based on different size fractions gives a means of rationalising key mechanisms and factors driving sediment loss in large river basins.

But, the confluence-based approach to source tracing does not separate critical processes such as raindrop impact, sheet, interrill or rill / gully erosion. Human activities in the study area comprising dry-land farming (rain fed cultivation systems) and residential areas on steep slopes (Fig. 2b and c, respectively), are all drivers for increasing erosion and sediment export. Tillage on the local steep slopes, and the resulting destruction of any protective vegetation canopy enhances the risk of both sheet and rill erosion (Govers, 1991; Jin et al., 2007; Toy et al., 2002; Valcárcel et al., 2003). The sub-basins that were identified by the fingerprinting exercise as the main spatial sources of fine-grained sediment in the study area comprise larger areas of dry-land farming on erodible lithologies. The conventional ploughing direction for local dry-land farming is up and down slope and this is also an important factor (Takken et al., 2001), especially on steep slopes, for increasing the velocity of surface runoff and the rates of soil particle detachment. In consequence, soil tillage management (Quine and Zhang, 2004) by ceasing land use change from rangeland to dry-land cultivation or at least changing conventional tillage practices to contour ploughing should be considered as soil erosion mitigation measures in the tributary sub-basins identified by the fingerprinting work. Over-grazing associated with leaving crop stubbles on farmland after harvesting enhances soil compaction, surface crusting and sealing, reduces soil porosity, soil organic matter, and consequently increases overland flow during rainfall events (Blanco-Canqui et al., 2006). So, maintaining the crop stubbles on the harvested soil surface, reducing grazing pressures, and adopting of no-till or minimum tillage on steep slope could be used to help increase resistance to soil erosion and sediment loss.

5. Conclusions

Data sparse regions like the mountainous areas of Iran lack fundamental evidence on sediment sources for understanding drainage basin sediment dynamics and targeting abatement strategies. Despite the difficult terrain in such areas, the confluence-based source fingerprinting approach provides a pragmatic basis for assembling new evidence which, in turn, is of interest to scientists and managers alike. There remains a need to test low-cost tracers in such settings to support wider uptake of fingerprinting techniques for filling evidence gaps in more data sparse regions. Future research projects could therefore test such tracers more strategically.

Declaration of Competing Interest

The authors declare that they have no known competing financial interests or personal relationships that could have appeared to influence the work reported in this paper.

Acknowledgements

Grant number 600.4346 funded the Iranian contribution to this work. KN has been funded to work at Water and Soil Resources Research, Institut für Geographie, Universität Augsburg, Germany by the Georg Forster Research Fellowships program, Alexander von Humboldt Foundation. ALC was supported by strategic funding from the UKRI (UK Research and Innovation) Biotechnology and Biological Sciences Research Council (BBSRC grant BBS/E/C/000I0330; Soil to Nutrition – project 3).

Appendix A. Supplementary material

Supplementary data to this article can be found online at https://doi.org/10.1016/j.catena.2021.105173.

References

Annells, R., et al., 1985. Geological map of Qazvin-Rasht Geological Survey of Iran. Geological Survey of Iran, Tehran.

Bahadori, M., et al., 2019. A novel approach of combining isotopic and geochemical signatures to differentiate the sources of sediments and particulate nutrients from different land uses. Sci. Total Environ. 655, 129–140.
Blanco-Canqui, H., Lal, R., Post, W.M., Izaurralde, R., Owens, L., 2006. Corn stover impacts on near-surface soil properties of no-till corn in Ohio. Soil Sci. Soc. Am. J. 70, 266–278.
Borrelli, P., et al., 2017. An assessment of the global impact of 21st century land use change on soil erosion. Nat. Commun. 8, 1–13.
Brosinsky, A., Foerster, S., Segl, K., Kaufmann, H., 2014. Spectral fingerprinting: sediment source discrimination and contribution modelling of artificial mixtures based on VNIR-SWIR spectral properties. J. Soils Sediments 14, 1949–1964.
Chen, F., Fang, N., Wang, Y., Tong, L., Shi, Z., 2017. Biomarkers in sedimentary sequences: Indicators to track sediment sources over decadal timescales. Geomorphology 278, 1–11.
Collins, A., et al., 2017. Sediment source fingerprinting as an aid to catchment management: a review of the current state of knowledge and a methodological decision-tree for end-users. J. Environ. Manage. 194, 86–108.
Collins, A., Walling, D., 2007. Sources of fine sediment recovered from the channel bed of lowland groundwater-fed catchments in the UK. Geomorphology 88, 120–138.
Collins, A., Walling, D., Leeks, G., 1996. Composite fingerprinting of the spatial source of fluvial suspended sediment: a case study of the Exe and Severn River basins, United Kingdom. Géomorphologie: Relief Processus. Environnement 2, 41–53.
Collins, A., Walling, D., Leeks, G., 1997a. Source type ascription for fluvial suspended sediment based on a quantitative composite fingerprinting technique. Catena 29, 1–27.
Collins, A., et al., 2012. Sediment source tracing in a lowland agricultural catchment in southern England using a modified procedure combining statistical analysis and numerical modelling. Sci. Total Environ. 414, 301–317.
Collins, A.L., et al., 2020. Sediment source fingerprinting: benchmarking recent outputs, remaining challenges and emerging themes. J. Soils Sediments.
Collins, A.L., Walling, D.E., 2004. Documenting catchment suspended sediment sources: problems, approaches and prospects. Prog. Phys. Geogr. 28, 159–196.
Collins, A.L., Walling, D.E., Leeks, G.J., 1997b. Fingerprinting the origin of fluvial suspended sediment in larger river basins: combining assessment of spatial provenance and source type. Geografiska Annaler: Series A. Physical Geography 79, 239–254.
D'Haen, K., Dusar, B., Verstraeten, G., Degryse, P., De Brue, H., 2013. A sediment fingerprinting approach to understand the geomorphic coupling in an eastern Mediterranean mountainous river catchment. Geomorphology 197, 64–75.
Davies, J., Olley, J., Hawker, D., McBroom, J., 2018. Application of the Bayesian approach to sediment fingerprinting and source attribution. Hydrol. Process. 32, 3978–3995.
Devereux, O.H., Prestegaard, K.L., Needelman, B.A., Gellis, A.C., 2010. Suspended sediment sources in an urban watershed, Northeast Branch Anacostia River, Maryland. Hydrol. Process. 24, 1391–1403.
Duerdoth, C., et al., 2015. Assessment of a rapid method for quantitative reach-scale estimates of deposited fine sediment in rivers. Geomorphology 230, 37–50.
Evrard, O., et al., 2019. Using spectrocolourimetry to trace sediment source dynamics in coastal catchments draining the main Fukushima radioactive pollution plume (2011–2017). J. Soils Sediments 19, 3290–3301.
Furuichi, T., et al., 2016. Paired geochemical tracing and load monitoring analysis for identifying sediment sources in a large catchment draining into the Great Barrier Reef Lagoon. Geomorphology 266, 41–52.
Garzanti, E., Wang, J.-G., Vezzoli, G., Limonta, M., 2016. Tracing provenance and sediment fluxes in the Irrawaddy River basin (Myanmar). Chem. Geol. 440, 73–90.
Gaspar, L., Blake, W.H., Smith, H.G., Lizaga, I., Navas, A., 2019. Testing the sensitivity of a multivariate mixing model using geochemical fingerprints with artificial mixtures. Geoderma 337, 498–510.
Gellis, A.C., Fuller, C.C., Van Metre, P.C., 2017. Sources and ages of fine-grained sediment to streams using fallout radionuclides in the Midwestern United States. J. Environ. Manage. 194, 73–85.
Govers, G., 1991. Rill erosion on arable land in central Belgium: rates, controls and predictability. Catena 18, 133–155.
Grygar, T.M., Popelka, J., 2016. Revisiting geochemical methods of distinguishing natural concentrations and pollution by risk elements in fluvial sediments. J. Geochem. Explor. 170, 39–57.
Guerra, A.J.T., Fullen, M.A., Jorge, M.d.C.O., Bezerra, J.F.R., Shokr, M.S., 2017. Slope processes, mass movement and soil erosion: A review. Pedosphere, 27, 27-41.
Habibi, S., Gholami, H., Fathabadi, A., Jansen, J.D., 2019. Fingerprinting sources of reservoir sediment via two modelling approaches. Sci. Total Environ. 663, 78–96.
Haddadchi, A., Olley, J., Laceby, P., 2014. Accuracy of mixing models in predicting sediment source contributions. Sci. Total Environ. 497–498, 139–152.
Haddadchi, A., Ryder, D.S., Evrard, O., Olley, J., 2013. Sediment Fingerprinting in Fluvial Systems: Review of Tracers, Sediment Sources and Mixing Models. Int. J. Sedim. Res. 28.
Horowitz, A.J., 1991. Primer on sediment-trace element chemistry. Lewis Publishers.
Horowitz, A.J., Stephens, V.C., Elrick, K.A., Smith, J.J., 2012. Concentrations and annual fluxes of sediment-associated chemical constituents from conterminous US coastal rivers using bed sediment data. Hydrol. Process. 26, 1090–1114.
Huggett, R.J., 2011. Fundamentals of Geomorphology, Third ed. Routledge, New York.
Hughes, A.O., Olley, J.M., Croke, J.C., McKergow, L.A., 2009. Sediment source changes over the last 250 years in a dry-tropical catchment, central Queensland, Australia. Geomorphology 104, 262–275.
Jin, K., et al., 2007. Effects of different management practices on the soil–water balance and crop yield for improved dryland farming in the Chinese Loess Plateau. Soil Tillage Res. 96, 131–144.
Koiter, A.J., et al., 2013. Investigating the role of connectivity and scale in assessing the sources of sediment in an agricultural watershed in the Canadian prairies using sediment source fingerprinting. J. Soils Sediments 13, 1676–1691.
Laceby, J.P., et al., 2017. The challenges and opportunities of addressing particle size effects in sediment source fingerprinting: A review. Earth Sci. Rev. 169, 85–103.
Loughran, R.J., Campbell, B.L., 1995. The identification of catchment sediment sources. In: Foster, I.D.L., Gurnell, A.M., Webb, B.W. (Eds.), Sediment and Water Quality in River Catchments. Wiley, Chichester, pp. 189–205.
Miller, J.R., Mackin, G., Miller, S.M.O., 2015. Application of geochemical tracers to fluvial sediment. Springer.
Minella, J.P.G., Walling, D.E., Merten, G.H., 2008. Combining sediment source tracing techniques with traditional monitoring to assess the impact of improved land management on catchment sediment yields. J. Hydrol. 348, 546–563.
Mohammadi Raigani, Z., Nosrati, K., Collins, A.L., 2019. Fingerprinting sub-basin spatial sediment sources in a large Iranian catchment under dry-land cultivation and rangeland farming: Combining geochemical tracers and weathering indices. J. Hydrol.: Reg. Stud. 24, 100613.
Nosrati, K., 2017. Ascribing soil erosion of hillslope components to river sediment yield. J. Environ. Manage. 194, 63–72.
Nosrati, K., Collins, A.L., 2019a. Fingerprinting the contribution of quarrying to fine-grained bed sediment in a mountainous catchment. Iran. River Res. Appl. 35, 290–300.
Nosrati, K., Collins, A.L., 2019b. Investigating the importance of recreational roads as a sediment source in a mountainous catchment using a fingerprinting procedure with different multivariate statistical techniques and a Bayesian un-mixing model. J. Hydrol. 569, 506–518.
Nosrati, K., Collins, A.L., Madankan, M., 2018. Fingerprinting sub-basin spatial sediment sources using different multivariate statistical techniques and the Modified MixSIR model. Catena 164, 32–43.
Nosrati, K., Fathi, Z., Collins, A.L., 2019. Fingerprinting sub-basin spatial suspended sediment sources by combining geochemical tracers and weathering indices. Environ. Sci. Pollut. Res. 26, 28401–28414.
Nosrati, K., et al., 2011. An exploratory study on the use of enzyme activities as sediment tracers: biochemical fingerprints? Int. J. Sedim. Res. 26, 136–151.
Nosrati, K., Govers, G., Semmens, B.X., Ward, E.J., 2014. A mixing model to incorporate uncertainty in sediment fingerprinting. Geoderma 217, 173–180.
Olley, J., Brooks, A., Spencer, J., Pietsch, T., Borombovits, D., 2013. Subsoil erosion dominates the supply of fine sediment to rivers draining into Princess Charlotte Bay, Australia. J. Environ. Radioact. 124, 121–129.
Othman, F., Sadeghian, M.S., Ebrahimi, F., Heydari, M., 2013. A study on sedimentation in Sefidroud Dam by using depth evaluation and comparing the results with USBR and FAO methods, 2nd International Conference on Environment, Energy and Biotechnology. doi, pp. 43-48.
Owens, P., et al., 2016. Fingerprinting and tracing the sources of soils and sediments: Earth and ocean science, geoarchaeological, forensic, and human health applications. Earth Sci. Rev. 162, 1–23.
Palazón, L., et al., 2015. Comparing catchment sediment fingerprinting procedures using an auto-evaluation approach with virtual sample mixtures. Sci. Total Environ. 532, 456–466.
Palazón, L., Navas, A., 2017. Variability in source sediment contributions by applying different statistic test for a Pyrenean catchment. J. Environ. Manage. 194, 42–53.
Pimentel, D., Burgess, M., 2013. Soil erosion threatens food production. Agriculture 3, 443–463.
Queavuviller, P., 1998. Operationally defined extraction procedures for soil and sediment analysis. 1 Standardisation. Trends Anal. Chem 17, 289–298.
Quine, T., Zhang, Y., 2004. Re-defining tillage erosion: quantifying intensity–direction relationships for complex terrain: 1. Derivation of an adirectional soil transport coefficient. Soil Use Manag. 20, 114–123.
Sanisaca, L.E.G., Gellis, A.C., Lorenz, D.L., 2017. Determining the sources of fine-grained sediment using the sediment source assessment tool (Sed_SAT). US Geological Survey, 2331–1258.
Senger, Ö., 2013. A statistical power comparison of the Kolmogorov-Smirnov two-sample test and the Wald Wolfowitz test in terms of fixed skewness and fixed kurtosis in large sample Sizes. Chinese Business Rev. 12, 469–476.
Stone, M., Collins, A., Silins, U., Emelko, M., Zhang, Y., 2014. The use of composite fingerprints to quantify sediment sources in a wildfire impacted landscape, Alberta, Canada. Sci. Total Environ. 473, 642–650.
Takken, I., et al., 2001. Effects of tillage on runoff and erosion patterns. Soil Tillage Res. 61, 55–60.
Tang, Q., et al., 2019. Fingerprinting the sources of water-mobilized sediment threatening agricultural and water resource sustainability: Progress, challenges and prospects in China. Science China Earth Sciences 1–14.
Thomas, M.F., 1994. Geomorphology in the tropics: a study of weathering and denudation in low latitudes. John Wiley & Sons.
Tiecher, T., Caner, L., Minella, J.P.G., Dos Santos, D.R., 2015. Combining visible-based-color parameters and geochemical tracers to improve sediment source discrimination and apportionment. Sci. Total Environ. 527, 135–149.
Toy, T.J., Foster, G.R., Renard, K.G., 2002. Soil Erosion: Processes, Prediction, Measurement, and Control. John Wiley & Sons.
Uber, M., et al., 2019. Comparing alternative tracing measurements and mixing models to fingerprint suspended sediment sources in a mesoscale Mediterranean catchment. J. Soils Sediments 19, 3255–3273.
Upadhayay, H.R., et al., 2020. Sensitivity of source apportionment predicted by a Bayesian tracer mixing model to the inclusion of a sediment connectivity index as an informative prior: Illustration using the Kharka catchment (Nepal). Sci. Total Environ. 136703.

Valcárcel, M., Taboada, M.T., Paz, A., Dafonte, J., 2003. Ephemeral gully erosion in northwestern Spain. Catena 50, 199–216.
Vale, S., Fuller, I., Procter, J., Basher, L., Smith, I., 2016. Application of a confluence-based sediment-fingerprinting approach to a dynamic sedimentary catchment, New Zealand. Hydrol. Process. 30, 812–829.
Walling, D., 2005. Tracing suspended sediment sources in catchments and river systems. Sci. Total Environ. 344, 159–184.
Walling, D., 2013. The evolution of sediment source fingerprinting investigations in fluvial systems. J. Soils Sediments 13, 1658–1675.
Walling, D., Collins, A., 2008. The catchment sediment budget as a management tool. Environ. Sci. Policy 11, 136–143.
Walling, D., Foster, I.D., 2016. Using environmental radionuclides and sediment geochemistry for tracing and dating fine fluvial sediment. In: Kondolf, G.M., Piégay, H. (Eds.), Tools in Fluvial Geomorphology. Wiley, Chichester, pp. 183–209.
Walling, D.E., Collins, A.L., 2016. Fine sediment transport and management. In: Gilvear, D.J., Greenwood, M.T., Thoms, M.C., Wood, P.J. (Eds.), River Science: Research and Management for the 21st Century. Wiley, London, pp. 37–60.
Walling, D.E., Owens, P.N., Leeks, G.J., 1998. The role of channel and floodplain storage in the suspended sediment budget of the River Ouse, Yorkshire, UK. Geomorphology 22, 225–242.
Walling, D.E., Owens, P.N., Leeks, G.J., 1999. Fingerprinting suspended sediment sources in the catchment of the River Ouse, Yorkshire, UK. Hydrol. Process. 13, 955–975.
Wilkes, M.A., et al., 2019. Physical and biological controls on fine sediment transport and storage in rivers. Wiley Interdisciplinary Rev. Water 6, e1331.
Zhang, Y., Collins, A., Horowitz, A., 2012. A preliminary assessment of the spatial sources of contemporary suspended sediment in the Ohio River basin, United States, using water quality data from the NASQAN programme in a source tracing procedure. Hydrol. Process. 26, 326–334.